ADVANCED MATERIALS
www.advmat.de

Materials Views
www.MaterialsViews.com

Triple Emulsion Drops with An Ultrathin Water Layer: High Encapsulation Efficiency and Enhanced Cargo Retention in Microcapsules

*Chang-Hyung Choi, Hyomin Lee, Alireza Abbaspourrad, June Hwan Kim, Jing Fan, Marco Caggioni, Chris Wesner, Taotao Zhu, and David A. Weitz**

Emulsions have been widely used as carriers for food, drugs, and cosmetics due to their great capability of encapsulation.[1,2] While they are typically produced by bulk emulsification,[3,4] recent advances in microfluidics enable precise control of multiphasic flows, leading to highly monodisperse emulsions with fine-tunable size, morphologies, and properties of each compartment.[5–10] For example, we can generate double emulsion drops with an additional intermediate phase that separates the innermost drop from continuous phase, providing highly efficient encapsulation of hydrophilic or hydrophobic cargos while avoiding cross-contamination.[11–13] Even more flexibility can be achieved by consolidation of the intermediate phase in double emulsion drops to form polymeric microcapsules, vesicles, and colloidosomes;[14–16] for instance, polymeric shell in microcapsules can be fine-tuned to facilitate controlled release to active cargo. Since many applications require the capsules to be dispersed in an aqueous phase, double emulsion-templated capsules are particularly suitable for encapsulation of hydrophilic cargo. However, for hydrophobic cargos protected by hydrophilic shells, we need an additional step to redisperse the capsules into an aqueous phase. Although microcapsules with perfluoropolyether shells reported recently allow cargo diversity and enhanced cargo retention, their application is limited by the cost and mechanical property of the shell.[17] Thus, there remains an unmet need for production of microcapsules that not only can provide long-term storage of hydrophobic cargo but also retain high encapsulation efficiency.

Here, we present triple emulsion drops with an ultrathin water layer in a single step microfluidic emulsification, to achieve high encapsulation efficiency of hydrophobic cargo in polymeric microcapsules. A water-in-oil biphasic flow confined in an injection capillary coflows with a hydrophobic photocurable oil phase, which are then emulsified by additional continuous aqueous phase, resulting in monodisperse triple emulsion drops with ultrathin intermediate water layers in dripping mode. This allows us to encapsulate hydrophobic cargo with high efficiency by minimizing the specific volume occupied by the ultrathin water layer. Moreover, we demonstrate that the ultrathin water layer can be further tailored by adding hydrogel precursor; the polymerized hydrogel shell provides a physical barrier that separates the hydrophobic cargo from directly contacting the polymer shell. This hydrogel shell enables enhanced retention of highly volatile small organic compounds (α-pinene) that are known to be very challenging;[18,19] low molecular weight molecules have high mobility and thus quickly diffuse through the shell.

To make triple emulsion drops with the ultrathin water layer, we use a glass capillary microfluidic device comprised of two tapered circular capillaries inserted into a square capillary. We use 2-[methoxy(polyethyleneoxy)propyl] trimethoxysilane (PEG-silane) to make the circular capillary wall hydrophilic. In addition, a small tapered capillary is inserted into the injection capillary to facilitate simultaneous injection of two immiscible fluids. Another circular capillary is inserted into the square capillary at the other side to confine the flow near the injection tip, thereby increasing the flow velocity; this is also treated with PEG-silane to make the capillary wall hydrophilic, as schematically illustrated in **Figure 1**a.

An oil phase is injected through the small tapered capillary to form the innermost drop. An aqueous phase is injected through the injection capillary. The coinjection of these two immiscible fluids results in an stream of plug-like oil drop due to strong affinity of the aqueous phase to polyethylene glycol (PEG)-treated injection capillary; the local confinement of oil-in-water biphasic flow near a tip of the injection capillary reduces deformation of the interface and effectively squeeze up to form the lubricated water layer between the plug-like water drop and the inner wall of the injection capillary, facilitating formation of the thin water layer.[20] We use a photocurable solution for the second oil phase and inject through the interstices of the square and injection capillaries from the same side with the injection capillary. Additional aqueous phase is injected through the square capillary from the other side as the continuous phase. The stream of plug-like oil drop from the injection

Dr. C.-H Choi, Dr. H. Lee, J. H. Kim, Dr. J. Fan, Prof. D. A. Weitz
Department of Physics
School of Engineering and Applied Sciences
Harvard University
Cambridge, MA 02138, USA
E-mail: weitz@seas.harvard.edu
Prof. A. Abbaspourrad
Department of Food Science
Cornell University
Ithaca, NY 14853, USA
Dr. M. Caggioni, C. Wesner, Dr. T. Zhu
Corporate Engineering
The Procter and Gamble
OH 45069, USA

DOI: 10.1002/adma.201505801

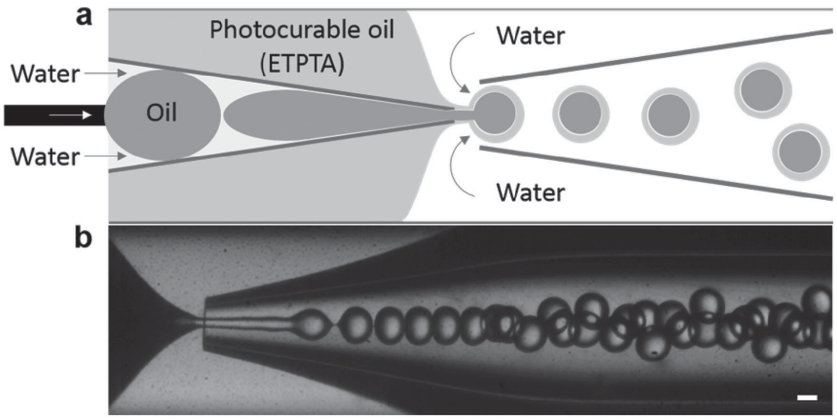

Figure 1. a) Microfluidic capillary device for production of oil-in-water-in-oil-in-water (o/w/o/w) triple emulsion drops with an ultrathin intermediate water layer. b) Optical microscope image showing formation of the triple emulsions in collection capillary. Scale bar represents 50 μm.

capillary coflows with the photocurable oil phase, which are emulsified by the continuous aqueous phase at the exit of the injection one, resulting in monodisperse triple emulsion drops with the ultrathin water layer. These emulsion drops then flow downstream through the collection capillary, as shown in the optical image of Figure 1b.

The ultrathin water layer in the triple emulsion drop separates the innermost oil phase from the photocurable oil phase making up the shell, enabling encapsulation of hydrophobic cargo within a miscible hydrophobic shell. Furthermore, minimizing the volume occupied by this water layer increases loading capacity of the hydrophobic cargo within the emulsion drops. To validate our approach, we use a model fragrance (α-pinene, Sigma–Aldrich) for the innermost oil phase (Q_1), an aqueous solution of 2% poly(vinyl alcohol) (PVA) for the ultrathin water layer (Q_2), photocurable ethoxylated trimethylolpropane triacrylate (ETPTA) as the second oil phase (Q_3), and aqueous solution of 10% PVA as the continuous phase (Q_4). To produce polymeric microcapsules, the stream of triple emulsion drops is exposed to UV illumination; this results in polymerization of the ETPTA monomer thereby forming a solid shell. The resulting microcapsules are monodisperse with coefficient of variation of 2%, as shown in the size distribution curve in **Figure 2**a,b. To distinguish each layer within the microcapsules, we label the ultrathin water layer with fluorescein sodium salt (green) and the innermost oil phase with Nile red (red). The microcapsules with an ultrathin water layer separating the polymeric shell and the innermost oil phase, are shown in confocal images of Figure 2c–e. Due to the optical resolution limit, it is impossible to measure the thickness of the ultrathin water layer using image analysis. Instead, we rupture the triple emulsion drops prior to the UV exposure to form two separated oil drops of the ETPTA and the innermost oil phase, as shown in bright-field images in Figure S1 in the Supporting Information. Then, we measure the volume of innermost oil drop and subtract it from the total volume of the triple emulsion drop. This gives us the volume initially occupied by the ultrathin water layer in the triple emulsion drop. Based on this measurement, the thickness of the ultrathin water layer is ≈650 nm; therefore, the encapsulation efficiency of the hydrophobic cargo is estimated to be above 95%. We also tune the polymeric shell thickness by adjusting the flow rate of the photocurable oil phase (Q_3), as evidenced by capsules with different shell thicknesses in bright-field images of Figure 2f. Importantly, while the thickness of the polymeric shell varies depending on the flow rate of Q_3, that of the ultrathin water layer is not affected by the flow rate of each phase, as shown in a plot of the shell thickness versus Q_3 of Figure 2g. This flow rate independence of the thickness of the water layer is attributed to the lubricated volume of water that preferentially wets the inner wall of the injection capillary.[20]

While triple emulsion drops with the ultrathin water layer enable high encapsulation efficiency of the hydrophobic model fragrance, the density mismatch between the fragrance and the ultrathin water layer ($\rho_{\text{fragrance}} = 0.858$ and $\rho_{2\%\ \text{PVA}} = 1.01$) results in the fragrance drop rising and directly contacting the inner surface of the polymeric shell; the hydrophobic fragrance imbibes into the hydrophobic polymer, leading to a rapid leakage and hence limiting the long-term storage. To achieve long-term storage of the fragrance, we tailor the formulation of the ultrathin water layer by rigidifying the ultrathin water layer, enabling it to act as a physical barrier and preventing direct exposure of the innermost fragrance with the polymeric shell. To demonstrate our strategy, we use triple emulsion drops with a water layer composed of an aqueous solution of 15% PEG diacrylate (PEG-DA, $M_n = 700$) with or without photoinitiator. In the presence of photoinitiator, PEG-DA precursor solution can be rapidly polymerized upon UV exposure, transforming into an ultrathin hydrogel layer. To investigate the effect of a thin water layer composition in enhanced cargo retention, we disperse the capsules into an aqueous solution and monitor the leakage behavior of fragrance using a bright-field microscope, as shown in bright-field images of **Figure 3**.

As a control experiment, we first test microcapsules with the ultrathin layer composed of 2% PVA; these microcapsules lead to rapid leakage of fragrance through polymeric membrane. The subsequent volume loss of the fragrance causes the shell to buckle within 24 h, as shown in bright-field images of Figure 3a. As we expected, the fragrance drop surrounded by the ultrathin water layer rises and directly contact the polymeric membrane, resulting in rapid leakage of the fragrance through the membrane. However, by using triple emulsion drops with 15% PEG-DA with photoinitator, we create microcapsules with an ultrathin hydrogel layer which is surrounded by the solidified polymeric shell, thereby forming a hydrophilic–hydrophobic hybrid shell. The resulting microcapsules with such hybrid polymeric shells notably improve the retention of fragrance, whereas a nonpolymerized PEG-DA layer leads to a rapid release, as evidenced by buckled and intact polymeric shell in bright-field images of Figure 3b,c, respectively. The leakage behavior from a nonpolymerized PEG-DA layer is similar with that of the microcapsules with the ultrathin layer of aqueous solution of 2% PVA. This result indicates that the

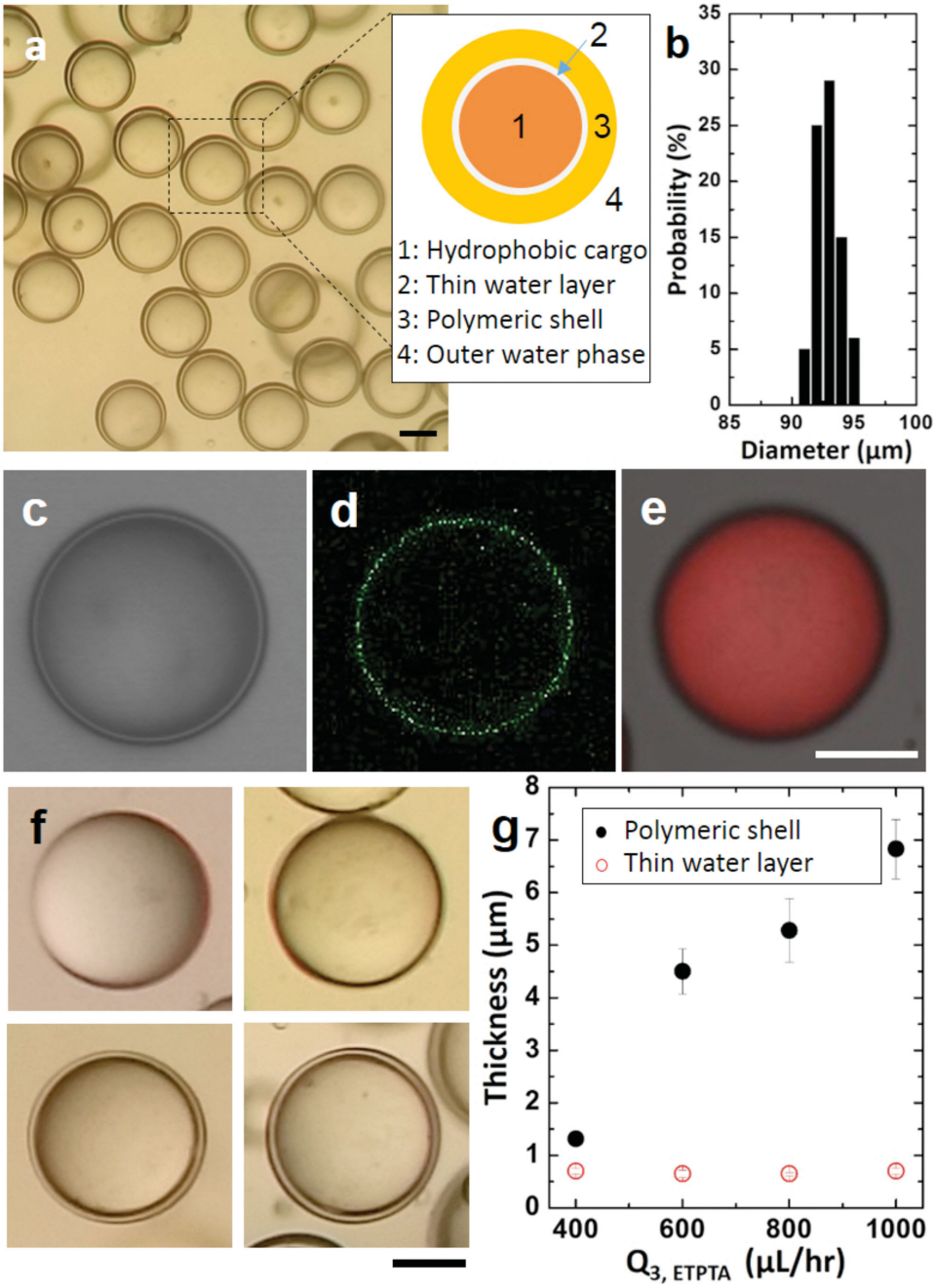

Figure 2. a) Bright-field microscope image of monodisperse microcapsules by photopolymerization of the triple emulsion drops. b) Size distribution of the triple emulsion drops. c–e) Optical and confocal images of polymeric microcapsules incorporating two fluorescent dyes; fluorescein (green) for the ultrathin water layer and Nile red (red) for the innermost oil phase. f) Bright-field images showing microcapsule with varying shell thickness, where Q_3 is varied from 400 to 1000 μL h^{-1}, and Q_1, Q_2, and Q_4 are maintained at 1000, 1500, and 15000 μL h^{-1}, respectively. g) Size of the shell thickness as a function of flow rate of the photocurable oil phase (Q_3), with a constant water layer thickness. Scale bars represent 50 μm.

ultrathin hydrogel layer effectively prevents fragrance from being exposed to the polymer shell; thus the resulting hybrid shells enable long-term storage of the fragrance. To test the long-term storage of fragrance in the microcapsules, we apply mechanical stress to rupture the polymeric capsules between two glass slides. A bright-field image exhibits the trace of fragrances released from the cracked polymeric shells, as shown in the bright-field image of Figure S2 in the Supporting Information. Although the hydrogel layer is very thin, it effectively suppresses the leakage of fragrance by separating them from the polymeric shell.

Using this triple emulsion approach, we achieve high encapsulation efficiency (≈95%) of hydrophobic cargo within a hydrophobic polymeric shell, which is difficult to achieve by conventional emulsification techniques. The thickness of the polymeric shell can be controlled by adjusting the flow rate

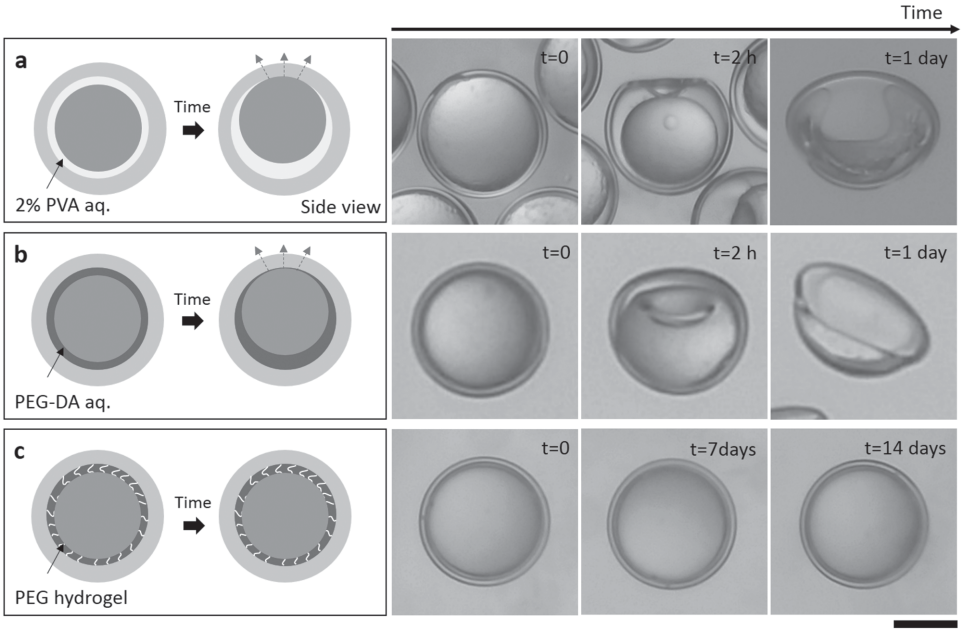

Figure 3. A series of bright-field microscope images showing the leakage of hydrophobic model fragrance (α-pinene) encapsulated in polymeric microcapsules, which is composed of a) 2% PVA aqueous solution, b) 15% PEG-DA aqueous solution, and c) PEG cross-linked hydrogel. The leakage behavior is monitored in an aqueous solution. Scale bar represents 50 μm.

of the photocurable oil phase while keeping the thickness of the ultrathin water layer constant; this approach enables consistent production of the microcapsules with high encapsulation efficiency. In addition, the ultrathin water layer can be formulated to rigidify into a cross-linked hydrogel, preventing direct exposure of the innermost oil drop from the shell while forming a hydrophilic–hydrophobic hybrid polymeric shell; thus this hybrid shell confers efficient diffusion barrier, allowing long-term storage of volatile hydrophobic cargo. Furthermore, this approach is not limited to a single type of hydrid polymeric shell but each shell composition can be tuned independently to create advanced functional microcapsules. For instance, the outer polymeric shell can be designed to disintegrate upon external stimuli such as pH- or temperature to achieve programmable release of encapsulated cargos.[21] Also, the ultrathin intermediate layer in the triple emulsion drops can be further tailored into omniphobic perfluorinated oil, enabling encapsulation of both hydrophilic and hydrophobic cargoes in a single emulsion template. The controllability and the versatility offered by this approach should be well-suited for high-end microencapsulation applications that mandates high encapsulation efficiency as well as high precision control over the physicochemical property of the microcapsules produced.

Experimental Section

Materials: PVA (89%–92% hydrolyzed, M_w 13 000–23 000), ethoxylated trimethylolpropane triacrylate, α-pinene, 2-hydroxy-2-methylpropiophenone, Nile red, and fluorescein sodium salt were purchased from Sigma–Aldrich Chemicals. 2-[methoxy(polyethyleneoxy)propyl] trimethoxy silane was obtained from Gelest, Inc. Glass capillaries were purchased from World Precision Instruments Inc. and AIT Glass, respectively. UV source (Omnicure S1000) was obtained from Lumen Dynamics.

Preparation of Microfluidic Device and Drop Generation: An injection capillary was prepared by tapering a circular glass capillary with 560 μm inner diameter to 40 μm inner diameter using a Sutter micropipette puller (P-97); to make the inner wall hydrophilic, it was dipped to 2-[methoxy(polyethyleneoxy)propyl] trimethoxy silane for 10 min and subsequently washed with deionized water (DI). The injection capillary was inserted into a square capillary whose inner width (1.05 mm) is slightly larger than that of the outer diameter of the injection capillary (1 mm). Next, a small tapered glass capillary (10 μm inner diameter) was prepared by heating and pulling a cylindrical capillary by hand using a gas torch; this capillary was inserted into the injection capillary for simultaneous injection of two immiscible fluids. Finally, a cylindrical collection capillary was inserted into the square capillary from the other end; this collection capillary was also treated with 2-[methoxy(polyethyleneoxy)propyl] trimethoxy silane to make the capillary wall hydrophilic. During drop generation, the volumetric flow rate was controlled by syringe pumps (Harvard Apparatus); flow rates of the innermost oil, thin-water layer, photocurable oil phase and continuous phase were typically set to be 1000, 1500, 1000, and 15 000 μL h^{-1}, respectively. The production of emulsion drops was observed using an inverted microscope equipped with a high-speed camera (Phantom V9.0).

Supporting Information

Supporting Information is available from the Wiley Online Library or from the author.

Acknowledgements

C.-H.C. and H.L. contributed equally to this work. J.H.K. is currently affiliated with Buckingham Browne and Nichols. This work was supported by Procter & Gamble Co., the National Science Foundation

(DMR-1310266), the Harvard Materials Research Science and Engineering Center (DMR-1420570), and the Basic Science Research Program through the National Research Foundation of Korea (NRF) funded by the Ministry of Education, Science and Technology (Grant No. 2013R1A6A3A03065122).

Received: November 23, 2015
Revised: January 6, 2016
Published online: March 2, 2016

[1] N. Garti, C. Bisperink, *Curr. Opin. Colloid Interface Sci.* **1998**, *3*, 657.
[2] S. Magdassi, N. Garti, *J. Colloid Interface Sci.* **1987**, *120*, 537.
[3] M. Nollet, M. Depardieu, M. Destribats, R. Backov, V. Schmitt, *Part. Part. Syst. Charact.* **2013**, *30*, 62.
[4] M. Depardieu, M. Nollet, M. Destribats, V. Schmitt, R. Backov, *Part. Part. Syst. Charact.* **2013**, *30*, 204.
[5] L.-Y. Chu, A. S. Utada, R. K. Shah, J.-W. Kim, D. A. Weitz, *Angew. Chem. Int. Ed.* **2007**, *119*, 9128.
[6] A. R. Abate, D. A. Weitz, *Small* **2009**, *5*, 2030.
[7] Z. Nie, S. Xu, M. Seo, P. C. Lewis, E. Kumacheva, *J. Am. Chem. Soc.* **2005**, *127*, 8058.
[8] A. S. Utada, E. Lorenceau, D. R. Link, P. D. Kaplan, H. A. Stone, D. A. Weitz, *Science* **2005**, *308*, 537.
[9] S. Okushima, T. Nisisako, T. Torii, T. Higuchi, *Langmuir* **2004**, *20*, 9905.
[10] D. Dendukuri, K. Tsoi, T. A. Hatton, P. S. Doyle, *Langmuir* **2005**, *21*, 2113.
[11] H. C. Shum, Y.-J. Zhao, S.-H. Kim, D. A. Weitz, *Angew. Chem. Int. Ed.* **2011**, *50*, 1648.
[12] M. Windbergs, Y. Zhao, J. Heyman, D. A. Weitz, *J. Am. Chem. Soc.* **2013**, *135*, 7933.
[13] C.-H. Choi, D. A. Weitz, C.-S. Lee, *Adv. Mater.* **2013**, *25*, 2536.
[14] D. Lee, D. A. Weitz, *Adv. Mater.* **2008**, *20*, 3498.
[15] H. C. Shum, D. Lee, I. Yoon, T. Kodger, D. A. Weitz, *Langmuir* **2008**, *24*, 7651.
[16] J.-W. Kim, A. S. Utada, A. Fernández-Nieves, Z. Hu, D. A. Weitz, *Angew. Chem. Int. Ed.* **2007**, *46*, 1819.
[17] M. A. Zieringer, N. J. Carroll, A. Abbaspourrad, S. A. Koehler, D. A. Weitz, *Small* **2015**, *11*, 2903.
[18] I. Hofmeister, K. Landfester, A. Taden, *Macromolecules* **2014**, *47*, 5768.
[19] J. E. Hawkins, G. T. Armstrong, *J. Am. Chem. Soc.* **1954**, *76*, 3756.
[20] S.-H. Kim, J. W. Kim, J.-C. Cho, D. A. Weitz, *Lab Chip* **2011**, *11*, 3162.
[21] A. Abbaspourrad, N. J. Carroll, S.-H. Kim, D. A. Weitz, *J. Am. Chem. Soc.* **2013**, *135*, 7744.